

# Improved Re-Crystallization of p<sup>+</sup> Poly-Si Gates with Molecular Ion Implantation

Jin-Ku Lee<sup>1</sup>, Min-Ae Ju<sup>1</sup>, Jae-Geun Oh<sup>1</sup>, Sun-Hwan Hwang<sup>1</sup>, Seung-Joon Jeon<sup>1</sup>,  
Ja-Chun Ku<sup>1</sup>, Sungki Park<sup>1</sup>, Kyung-Won Lee<sup>2</sup>, Steve Kim<sup>2</sup>, Geum-Joo Ra<sup>2</sup>,  
Ron Reece<sup>2</sup>, Leonard M. Rubin<sup>2</sup>, W. A. Krull<sup>3</sup>, and H. T. Cho<sup>3</sup>

<sup>1</sup>*Hynix Semiconductor Inc., San 136-1 Ami-ri, Bubal-eub, Ichon-si, Kyoungki-do, 467-701, Korea*

<sup>2</sup>*Axcelis Technologies Inc., 108 Cherry Hill Drive, Beverly, MA 01915, USA*

<sup>3</sup>*SemEquip Inc. 34 Sullivan Road, N.Billerica, MA 01862, USA*

**Abstract.** Implantation of B<sub>18</sub>H<sub>22</sub> molecules at 80 keV and doses up to 4x10<sup>16</sup>cm<sup>-2</sup> were evaluated for the application of p-type counterdoping of *in situ* n-type doped polysilicon gates. Compared to conventional B implants, molecular implantation provides greatly improved throughput without the risk of energy contamination. Implants at these high doses resulted in poor re-crystallization of the polysilicon layer due to the formation of excessive cluster-type defects. Subjecting the polysilicon to either UV-curing or low temperature soak annealing prior to dopant activation was not effective in improving the re-crystallization process. However, breaking the dose into two portions at two different energies was shown to significantly improve re-crystallization of the polysilicon layer. Improved dopant activation was confirmed by a >90% reduction in ring oscillator delay time on a 60 nm PMOSFET.

**Keywords:** Octadecaborane, Ion Implantation, Polysilicon Doping

**PACS:** 61.72.-y, 61.72.U-, 68.55.Ln, 85.40.Ry

## INTRODUCTION

Modern DRAM fabrication requires very high dose boron doping to form the p+ poly gate by counterdoping of an *in situ* n-type doped poly layer [1,2]. High doping is also required for low resistance shallow junction formation and bit line contact resistance improvement. However, traditional beam line implantation suffers from either low beam current in drift mode or energy contamination in deceleration mode. For very high dose implants (more than 4x10<sup>16</sup>cm<sup>-2</sup>), boron forms clusters near the projected range during annealing. These clusters prevent the damaged layer from achieving complete re-crystallization, and cannot be eliminated by additional thermal processing. The result is poor device electrical characteristics, especially ring oscillator (R/O) delay.

In order to improve the re-crystallization of the implanted layer, we studied B<sub>18</sub>H<sub>22</sub> molecular ion implantation process. For the same equivalent B energy, B<sub>18</sub>H<sub>22</sub> has the same projected range (Rp) but better dopant activation. This improved activation is demonstrated on a 60 nm PMOS device.

## EXPERIMENTAL

Initial work to measure the degree of re-crystallization was done on bare silicon wafers. We implanted B at energy of 5 keV and B<sub>18</sub>H<sub>22</sub> at 30 to 80 keV (1.6 to 4.2 keV B equivalent) and doses of 1x10<sup>15</sup>cm<sup>-2</sup> to 5x10<sup>16</sup>cm<sup>-2</sup>. After annealing, various thermal treatments were investigated. These include poly implant annealing (PIA) for 10 to 30 seconds at temperatures of 700 to 1000°C, low temperature annealing for 10 to 20 minutes at 500 to 600°C, UV curing at 400°C for 10 to 15 minutes, and PIA at 950 and 1000°C. Breaking the 4x10<sup>16</sup>cm<sup>-2</sup> dose into two implants, one at 80 keV and another at 30 to 50 keV was also investigated. The doping characteristics and surface morphologies were analyzed with secondary ion mass spectrometry (SIMS), transmission electron microscopy (TEM), and a conventional four point probe.

We then implanted B or B<sub>18</sub>H<sub>22</sub> at 30 to 80 KeV, 4x10<sup>16</sup>cm<sup>-2</sup>, into a 60 nm p+ poly gated device and measured the electrical characteristics including ring oscillator delay.

Figure 1 shows the processing sequence for these devices.

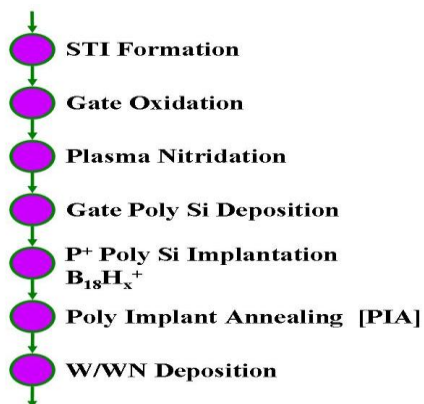


FIGURE 1. Process sequence for p+ poly-Si gate fabrication.

## RESULTS AND DISCUSSION

Figure 2 shows the doping profile and cross sectional TEM of a boron, 5 keV,  $4 \times 10^{16} \text{ cm}^{-2}$  implant annealed at  $950^\circ\text{C}$ . The boron has piled up at the projected range ( $\sim 130\text{\AA}$ ) after annealing, and the damaged layer could not be re-crystallized due to the heavily piled up boron dopants seen on the TEM image. This damage takes the form of boron-interstitial clusters [3].

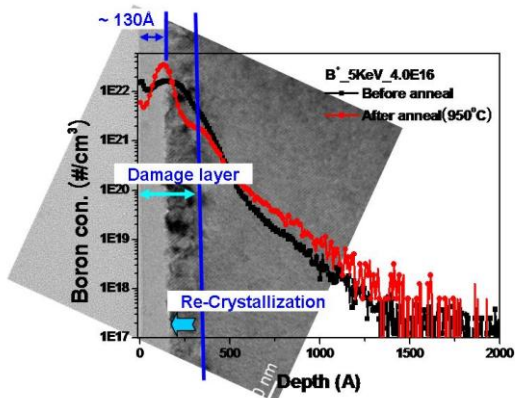
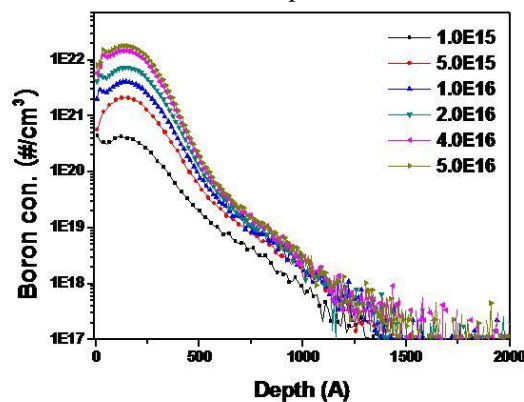


FIGURE 2. SIMS and cross sectional TEM for a B, 5 keV,  $4 \times 10^{16} \text{ cm}^{-2}$  implant annealed at  $950^\circ\text{C}$ .

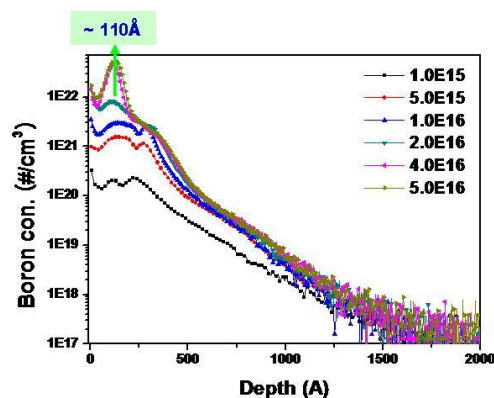
Figure 3 shows boron profiles for 80 keV  $\text{B}_{18}\text{H}_x^+$  ( $4.2 \text{ keV B}$  equivalent) at various doses before and after annealing at  $950^\circ\text{C}$ . The boron piled up at the projected range during the thermal treatment for all doses  $\geq 2 \times 10^{16} \text{ cm}^{-2}$ .

Figure 4 shows TEM images for  $2\text{--}4 \times 10^{16} \text{ cm}^{-2}$  doses before and after annealing. While the damaged layer at  $2 \times 10^{16} \text{ cm}^{-2}$  has been re-crystallized well, the

damaged layer (Figure 3,  $\sim 110\text{\AA}$ ) with  $4 \times 10^{16} \text{ cm}^{-2}$  couldn't be re-crystallized after annealing. This is similar to monomer boron implantation.



(a)



(b)

FIGURE 3. B profiles for 80 keV  $\text{B}_{18}\text{H}_x^+$  at various doses before (a) and after (b) annealing at  $950^\circ\text{C}$ .

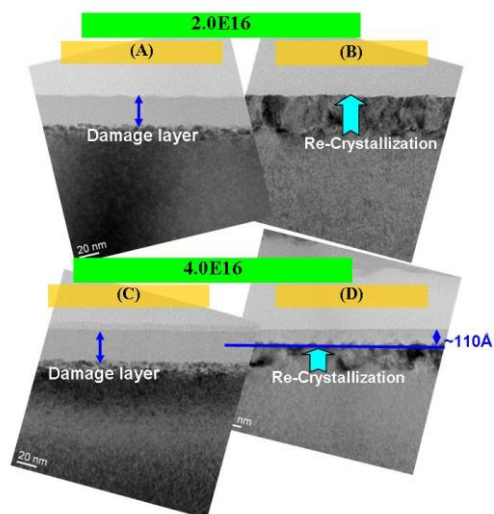
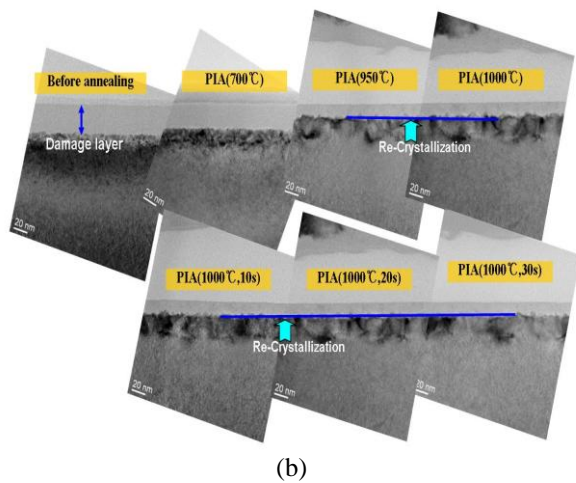
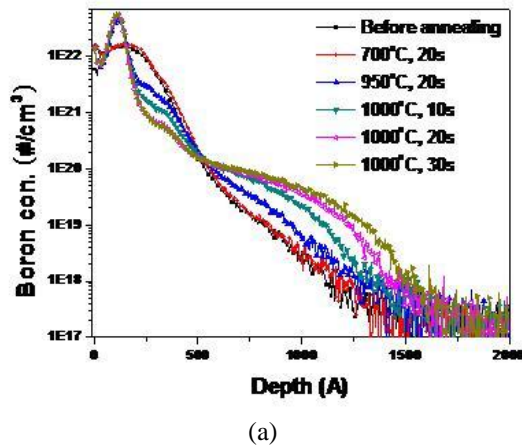


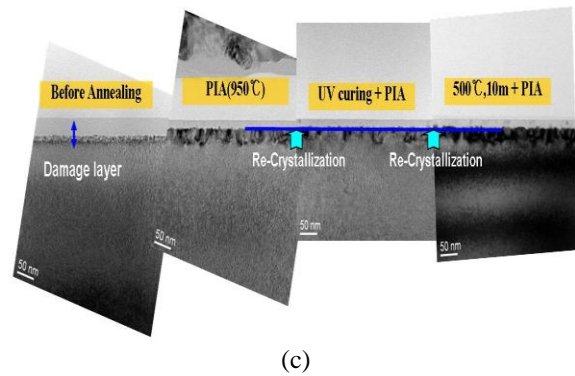
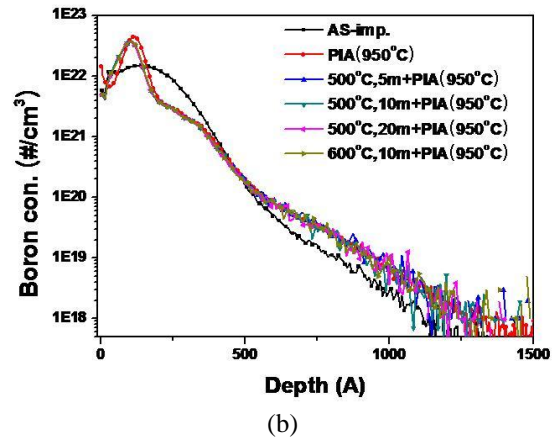
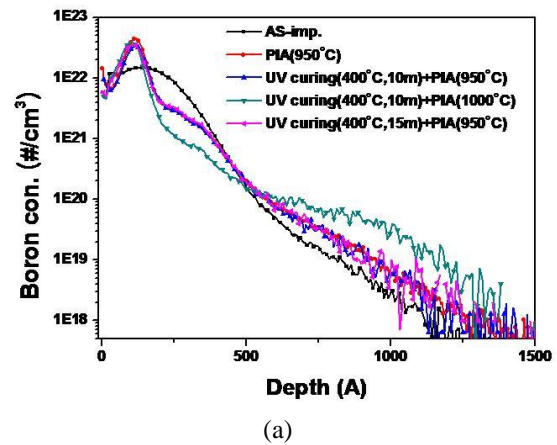
FIGURE 4. TEM images before and after annealing of (a,b)  $2 \times 10^{16} \text{ cm}^{-2}$  (c,d)  $4 \times 10^{16} \text{ cm}^{-2}$  dose.

Figure 5 shows SIMS and TEM data for 80 keV,  $4 \times 10^{16} \text{ cm}^{-2}$   $\text{B}_{18}\text{H}_x^+$  implants with various annealing conditions. The anneal temperatures are 700, 950, and 1000°C for 20 seconds. Additionally, there were anneals of 10 and 30 seconds at 1000°C. There were no indications of dopant movement or damage layer evolution for 700°C anneals. This temperature was too low to activate the dopants. All samples show boron pile up at Rp for anneals  $\geq 950^\circ\text{C}$ , with no re-crystallization of the damage layer visible by TEM



**FIGURE 5.** (a) SIMS profiles and (b) TEM images for 80 keV,  $4 \times 10^{16} \text{ cm}^{-2}$   $\text{B}_{18}\text{H}_x^+$  implants with various annealing conditions.

Figure 6 shows SIMS profiles and TEM images for 80 keV,  $4 \times 10^{16} \text{ cm}^{-2}$   $\text{B}_{18}\text{H}_x^+$  implants with UV curing and low temperature annealing before PIA. Pre-anneal treatments like UV-curing (Figure 6a) and low temperature annealing (Figure 6b) did not significantly affect the amount of boron pile up or the re-crystallization of the damage layer as indicated by TEM (Figure 6c).



**FIGURE 6.** SIMS profiles and TEM images for 80 keV,  $4 \times 10^{16} \text{ cm}^{-2}$   $\text{B}_{18}\text{H}_x^+$  implants with UV curing and low temperature annealing before PIA.

Figure 7 shows SIMS data for single step implants and when the dose is implanted at two different energies. The total dose was  $4 \times 10^{16} \text{ cm}^{-2}$  and the post-implant annealing was at 1000°C. The dopant profiles are different after annealing as the peak locations have shifted significantly. The amount of boron at the surface decreased for the two step implant process.

Figure 8 compares the damage layer before and after annealing for single implant and two energy

implants. The damage layer from the two step implant showed better recovery after annealing than the single implant step. This is attributed to reduced boron pileup at the projected range (Figure 7).

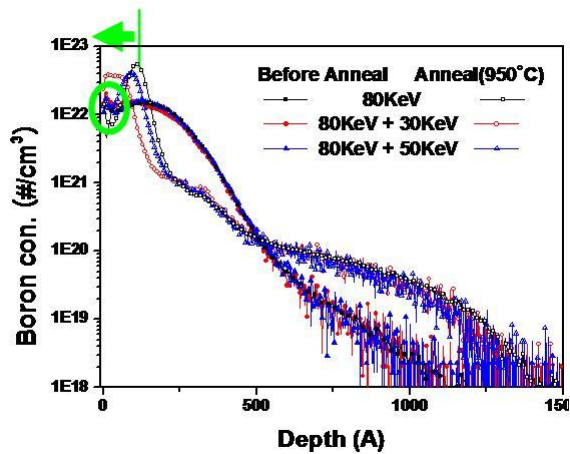


FIGURE 7. SIMS profiles of single energy and two energy implants. The total dose was  $4 \times 10^{16} \text{ cm}^{-2}$  in all cases.

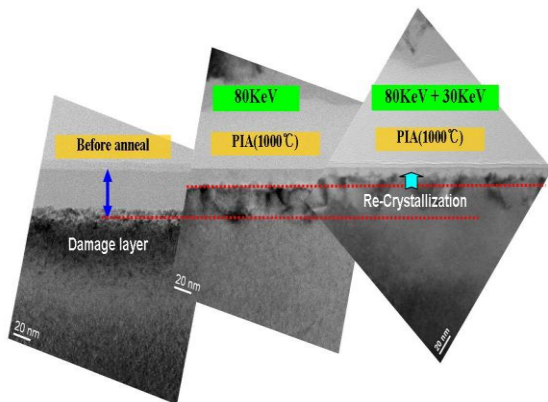


FIGURE 8. Comparison of implant damage layer before and after annealing for single implant and two energy implants.

Figure 9 shows the R/O delay results from a 60 nm PMOS device with the two step implant process. Breaking the dose into two different energies improved the R/O delay by over 90% as compared with a single high dose implantation.

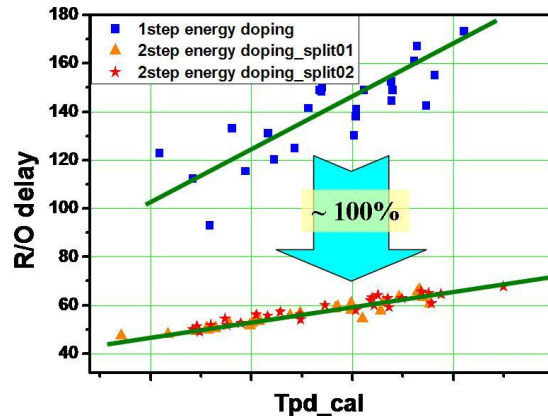


FIGURE 9. Ring oscillator delay results from 60 nm PMOS device.

## CONCLUSIONS

We improved the re-crystallization of the damage layer from a  $B_{18}H_x$  implant by breaking the high dose ( $\sim 4 \times 10^{16} \text{ cm}^{-2}$ ) into two implants at two different energies. The two step implant was shown to move the dopant pile up region closer to the surface without significantly changing the rest of the dopant profile. In addition to improved damage recovery in the near surface region, R/O delay was reduced by almost 100% in a 60 nm MOSFET.

## REFERENCES

1. S. H. Hwang, *et al.*, "Investigation of Converted p+ Poly-Si Gate Formed by  $B_{18}H_x$  Cluster Ion Implantation", in *Proceedings of the International Conference on Ion Implantation Technology*, 2006, pp. 163-166.
2. D. Henke, *et al.*, "P-Type Gate Electrode Formation Using  $B_{18}H_{22}$  Ion Implantation", in *Proceedings of the International Conference on Ion Implantation Technology* 2006, pp. 202-205.
3. S. Solmi, *et al.*, "Boron-interstitial silicon clusters and their effects on transient enhanced diffusion of boron in silicon", *J. Appl. Phys.* **88**, 4547 (2000).